

## Electronic structure of Sm monochalcogenides

B. Batlogg, E. Kaldis, A. Schlegel, and P. Wachter

*Laboratorium für Festkörperphysik, Eidgenössische Technische Hochschule Zürich, 8049 Zürich, Switzerland*

(Received 17 February 1976)

The optical reflectivity of single crystals of semiconducting SmS, SmSe, and SmTe as well as of the metallic, high-pressure phase of SmS has been investigated in the photon energy range between 0.03 and 12 eV, for metallic SmS also between 4.2 and 300 K. The dielectric functions have been derived by means of a Kramers-Kronig analysis and been interpreted by interband and intraband transitions. In addition, semiconducting evaporated films of SmS have been prepared and the absorption in function of temperature (4.2–300 K) and pressure (0–1.5 kbar) has been investigated. It can be shown that the electronic structure of the semiconducting Sm monochalcogenides can be obtained from the corresponding one of the Eu monochalcogenides by a simple uniform shift in the energy of the  $4f$  electronic state. Valence fluctuations in single crystalline, metallic SmS are present to a much lower degree than assumed so far.

### I. INTRODUCTION

In recent years the Sm monochalcogenides have received great attention by many scientists because of their interesting physical properties. After the first structure analysis of Picon and Patrie<sup>1</sup> and Picon *et al.*<sup>2</sup> the semiconducting properties of SmS were soon recognized.<sup>3–5</sup> Already in 1964 Zhuze *et al.*<sup>5</sup> mentioned that SmS acquired a golden surface color after polishing, which today can be taken as the first hint of a pressure-induced semiconductor-metal transition. A great number of papers followed, after Jayaraman *et al.* experimentally verified the pressure-induced phase transitions in the Sm monochalcogenides<sup>6</sup> and showed that it was first order in SmS at a critical pressure of only 6.5 kbar. Shortly thereafter the concept of valence fluctuations was applied to the high-pressure metallic phase of SmS to explain its nonmagnetic state.<sup>7,8</sup> In spite of the fact that the semiconductor-metal transition of SmS might be a proving ground for many modern theories, significant experiments on undoped, single-crystalline materials are scarce due to experimental difficulties with high-pressure work. Additional problems arising because of nonstoichiometry of the materials, measurements on powder samples, or using nonhydrostatic pressures are usually not realized and mostly underestimated. However, the recent work on Gd monochalcogenides has shown the tremendous influence of nonstoichiometry on the magnetical,<sup>9</sup> optical,<sup>10,11</sup> and electrical<sup>12,13</sup> properties of these compounds. Similar effects are also present in other rare-earth chalcogenides.

Hence, experimentally, it appeared to be a significant achievement that the metallic phase of SmS could be induced by chemical alloying with cations<sup>14–17</sup> of smaller size than  $\text{Sm}^{2+}$  or with trivalent anions<sup>18</sup> inducing  $\text{Sm}^{3+}$  ion formation. The lattice pressure was thus chemically induced, but addi-

tional problems arose owing to inhomogeneous distributions of substituents and the incorporation of their electrons. We think that chemical alloying does not simplify the problems and in some cases different results, as compared with the high-pressure experiments, are obtained.

The hypothesis of a fluctuating valence in the metallic phase of SmS was put on a new basis when x-ray photoelectron spectroscopy was applied to the chemically collapsed phase of SmS,<sup>18,19</sup> and an upper limit of  $10^{-16}$  sec has been set for the fluctuation time. A lower limit of  $10^{-9}$  sec is given by the Mössbauer studies on chemically collapsed SmS,<sup>20</sup> and on SmS under high pressure.<sup>21</sup>

In this paper we report the measurement of the optical properties of single crystals of the Sm monochalcogenides. We explain these properties and derive the electronic structure of the above compounds. This is also done for the metallic phase of SmS which has been obtained by polishing the surface of single crystals. This technique is practically (for the moment) the only way to obtain the optical constants over a photon range between 0.03 and 12 eV and at low temperatures. On the other hand semiconducting films of SmS have also been prepared and have been investigated at low temperatures and at pressures up to 1.5 kbar.

### II. CRYSTAL GROWTH

We have grown samarium-chalcogenide single crystals by high-temperature iodine transport and sublimation, from the melt and by recrystallization, in evacuated and sealed tungsten and molybdenum crucibles. Details of these growth methods have been given elsewhere.<sup>22</sup> For the particular measurements discussed in this paper crystals grown under the following conditions have been used:

- (a) SmS single crystals were grown by sublima-

tion in a very small temperature gradient  $\Delta T = 28^\circ\text{C}$  ( $2024 - 2052^\circ\text{C}$ ). Large single crystals of centimeter dimensions with lattice constant  $a = 5.9709 \pm 0.0004 \text{ \AA}$  were obtained. Variations of stoichiometry can be obtained, if desirable, in an experiment by combining melt growth and distillation of the melt in a sealed crucible. Crystals grown at the bottom of the crucible from the melt by directional solidification had a lattice constant  $a = 5.9694 \pm 0.0004 \text{ \AA}$ .

(b) SmSe single crystals were obtained by a similar combined experiment as described above. The crystals used in the present work were grown from the melt, which was overheated to  $2200^\circ\text{C}$  by directional solidification using a cooling rate of  $20^\circ\text{C/h}$ . The solidified melt contained regularly shaped single crystalline grains of dimension approximately  $7 \times 5 \times 5 \text{ mm}^3$  and parallel orientation. The lattice constant is  $a = 6.1975 \pm 0.0003 \text{ \AA}$ .

(c) SmTe single crystals with dimensions  $5 \times 4 \times 4 \text{ mm}^3$  were grown from the melt overheated to  $2090^\circ\text{C}$  by directional solidification.

### III. REFLECTIVITY AND KRAMERS-KRONIG ANALYSIS

The reflectivity of mechanically polished and annealed single crystals of SmS, SmSe, and SmTe has been measured at room temperature for photon energies between 0.03 and 12 eV. After polishing and prior to thermal annealing SmS obtained the well-known golden surface color typical of the metallic phase.<sup>5,6,23-26</sup> Microscopic investigation of the surface revealed that 15% of the surface consisted of untransformed, black and semiconducting SmS spots, randomly distributed within the metallic phase. Since the reflectivity of the semiconducting SmS phase is known from annealed samples, the reflectivity of a 100% transformed golden metallic surface can easily be computed. The reflectivity of semiconducting SmS, SmSe, SmTe, and metallic SmS is shown in Figs. 1-4. The curve for semiconducting SmS agrees very well with results of Güntherodt<sup>27</sup> and at room temperature we observe a reflectivity minimum in the far infrared at  $8.3 \mu\text{m}$  due to a coupled plasma resonance of the free charge carriers with LO phonons.<sup>23</sup> On the other hand our reflectivity values for SmS are at least a factor of 2 larger than the ones reported by Kirk *et al.*<sup>28</sup> Since the lattice constants, the ionic radii, and the atomic weights of the Eu and Sm chalcogenides are practically the same, we can add to our measured photon energy range the reflectivity of the residual ray bands of the Eu chalcogenides, measured by Axe<sup>29</sup> and Holah *et al.*<sup>30</sup>

The reflectivity of our polished metallic SmS

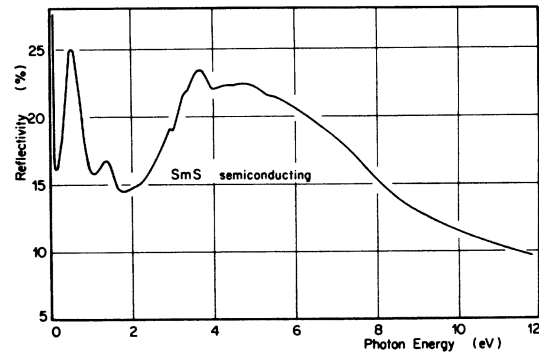


FIG. 1. Reflectivity of semiconducting SmS.

phase agrees qualitatively with the high-pressure measurement of Kirk *et al.*<sup>28</sup> However, we were able to show experimentally that the maximum in reflectivity reported by these authors<sup>28</sup> at about  $0.84 \mu\text{m}$  (1.5 eV) is caused by the comparison with an aluminum mirror, which has a well-known dip in its reflectivity at this energy. The reflectivity of our metallic SmS phase agrees very well with the one of a chemically collapsed  $\text{Sm}_{0.82}\text{Y}_{0.18}\text{S}$ ,<sup>31</sup> both in magnitude and in the energy of prominent features (minimum of reflectivity at 3.0 eV, kink at 4.1 eV).

In addition we have measured the reflectivity of the metallic phase of SmS as a function of temperature. The curve at 4.2 K is also shown in Fig. 2 and it is obvious that no shift of the reflectivity edge towards lower energy is observed upon lowering the temperature. On the contrary, the reflectivity edge becomes somewhat steeper, as is to be expected and as it is also found in the temperature dependence of the reflectivity of GdS. These measurements are in agreement with a statement by Pohl *et al.*<sup>32</sup> that the transmission

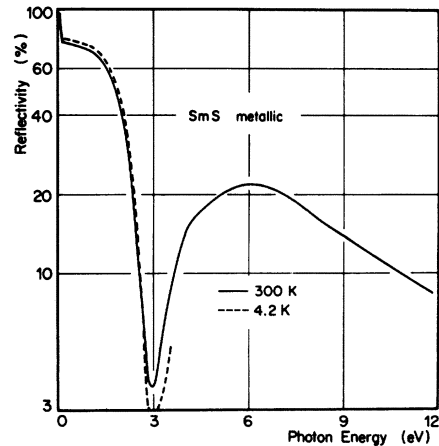


FIG. 2. Reflectivity of metallic SmS.

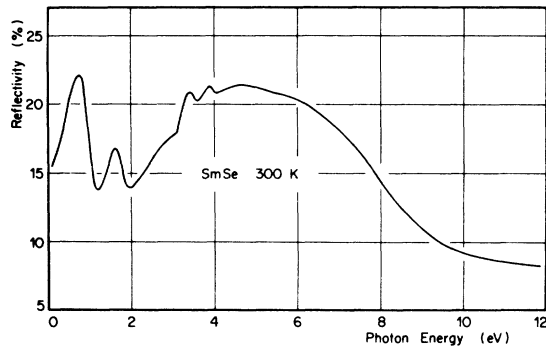


FIG. 3. Reflectivity of SmSe.

of metallic, polished SmS films did not change significantly upon cooling. On the other hand chemically collapsed  $\text{Sm}_{0.75}\text{Y}_{0.25}\text{S}$  does exhibit a remarkable shift of the reflectivity edge towards lower energies with decreasing temperature: the material reverts to the black phase.<sup>31</sup> Already now it may be stated that the pressure-induced metallic phase of SmS and the chemically collapsed metallic phase of SmS are not the same.

The reflectivity spectra shown in Figs. 1–4 have been analyzed in terms of the optical constants by means of the Kramers-Kronig (KK) relation. The reflectivity of the semiconducting Sm chalcogenides, completed by the residual ray spectrum of the corresponding Eu chalcogenides, now spans the energy range 0–12 eV. It has been extrapolated above 12 eV using a sequence of power laws of inverse frequency, just as in the case of the Eu chalcogenides.<sup>33</sup> The reflectivity of the metallic phase of SmS has been extrapolated to 100% for zero energy and for energies above 12 eV in the same way as for the Gd chalcogenides.<sup>11</sup> In Sec. IV the optical constants or the dielectric response function will be discussed in terms of interband transitions, coupled plasmon modes, and the properties of free conduction electrons.

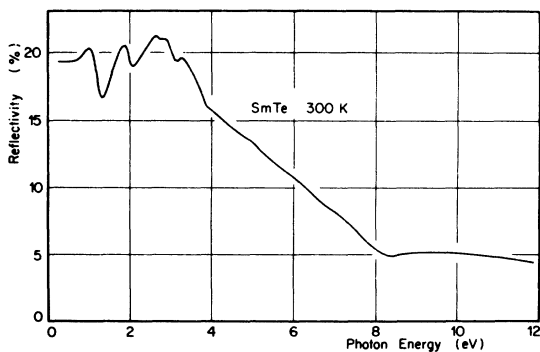


FIG. 4. Reflectivity of SmTe.

#### IV. INTERBAND TRANSITIONS

As a result of the KK analysis we have obtained the real and imaginary part of the dielectric function for the semiconducting phases of SmS, SmSe, and SmTe. They are shown in Figs. 5–7 within the spectral range of the interband transitions. If one observes electronic transitions from a localized  $4f^n$  shell, one has to consider that the remaining  $n-1$  electrons can be in excited states before relaxation with the lattice. This has already been found in the case of the Eu chalcogenides, where the  $4f^{n-1}$  state consists of a simple  ${}^7F_J$  multiplet.<sup>33</sup> In the Sm chalcogenides the  $4f^{n-1}$  state consists of three multiplets with the same multiplicity  $4f^5({}^6H_J, {}^6F_J, {}^6P_J)$  for a  $4f^6 \rightarrow 4f^5 5d$  transition. The probability to find the  $4f$  shell in one of these multiplets can be computed using the method of “coefficients of fractional parentage.”<sup>34</sup> The energy differences between the centers of gravity of the multiplets are also known from spectroscopic measurements.<sup>35</sup> In Figs. 5–7 the multiplets with their spectroscopic classification are shown in the inset. The height of the lines corresponds to the computed coefficients of fractional parentage. The cubic crystal field is splitting the  $5d$  conduction band in a lower-lying  $5d t_{2g}$  and a higher lying  $5d e_g$  sub-level. Optical  $4f^n \rightarrow 4f^{n-1} 5d$  transitions thus always appear twice and if the coordination of absorption peaks is made correctly, one obtains experimentally the crystal-field splitting of the  $5d$  states. In Figs. 5–7 the three  $4f^5$  multiplets are arranged at the bottom of the figures in such a way as to yield best agreement with the absorptive part of the dielectric function  $\epsilon_2$ . The crystal-field splitting of the  $5d$  states,  $\Delta_{CF}$ , is indicated in the figures. Besides  $4f^6 \rightarrow 5d$  transitions we also expect transitions from the  $p^6$  valence band of the anions into the crystal-field-split  $5d$  and possibly in  $6s$  bands. For example, in Fig. 5 we observe the  $3p^6 \rightarrow 5d t_{2g}$  transition at about 4.8 eV and the  $3p^6 \rightarrow 5d e_g$  transition barely indicated at about 7 eV, yielding

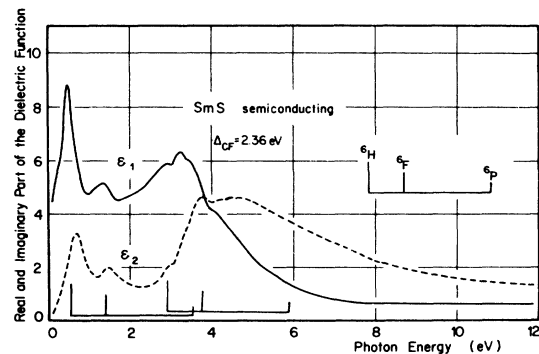


FIG. 5. Dielectric function of semiconducting SmS.

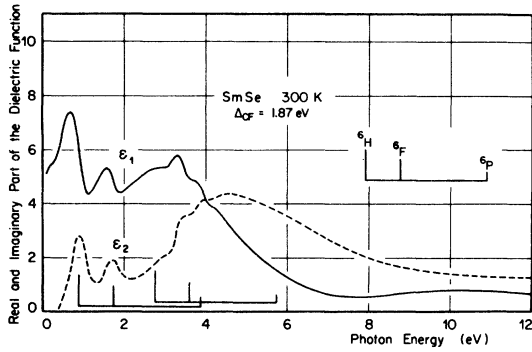


FIG. 6. Dielectric function of SmSe.

about the same crystal-field splitting  $\Delta_{CF}$  as observed for the  $4f^6 \rightarrow 5d$  transitions.

For metallic SmS the real and imaginary parts of the dielectric function have also been computed and are displayed in Fig. 8. In the infrared spectral region  $\epsilon_2$  decreases with increasing photon energy from very high positive values below 1 eV to a minimum at 3.1 eV. This minimum separates the region of "free electron" behavior from the region of interband transitions and it determines at the same time the low-energy limit of the latter.<sup>11</sup> A broad maximum in  $\epsilon_2$  due to interband transitions is found at 5.5 eV. Analogously to the well-studied Gd and La monochalcogenides<sup>11</sup> we assign this maximum to a transition from the  $3p^6$  anion valence band to empty conduction-band states above  $E_F$  (the Fermi energy). The presence of about one free electron per cation sufficiently screens the crystal field acting on the  $5d$  band so that no crystal-field splitting is observed experimentally.<sup>11</sup> Besides the maximum in  $\epsilon_2$  we are also observing a sharp kink at 4.5 eV, which in reality is a superimposed absorption peak. It corresponds to a  $4f^5(^6H_{5/2})$  transition of trivalent Sm to empty states above  $E_F$ .

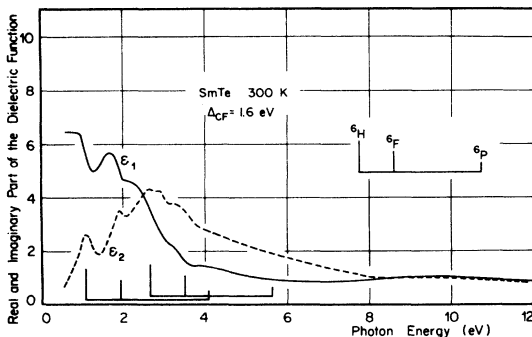


FIG. 7. Dielectric function of SmTe.

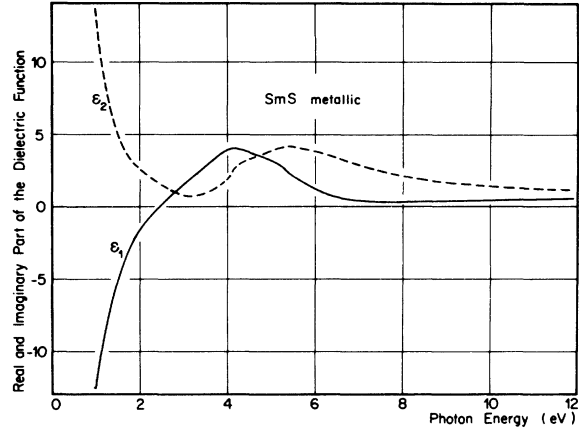
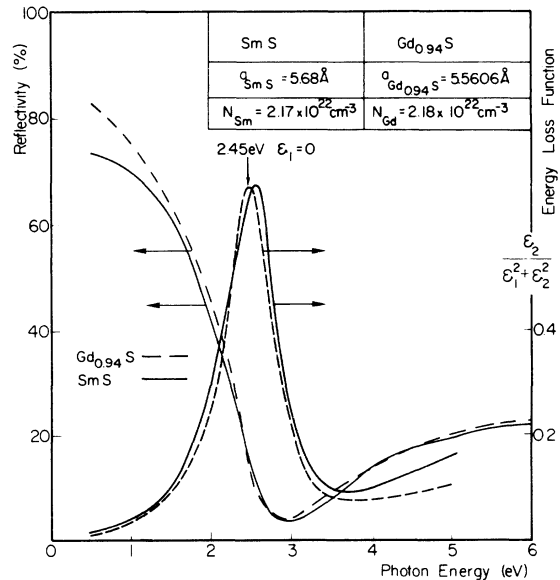


FIG. 8. Dielectric function of metallic SmS.

### V. PLASMON MODES IN METALLIC SmS

Starting from low energies in Fig. 8,  $\epsilon_1$  increases from very large negative values to a maximum at 4.2 eV. The intersection  $\epsilon_1 = 0$  with a positive slope at 2.45 eV clearly indicates a longitudinal excitation mode. If we compute the energy-loss function  $\epsilon_2 / (\epsilon_1^2 + \epsilon_2^2)$ , we obtain a pronounced maximum in the vicinity of  $\epsilon_1 = 0$ , owing to a coupled plasmon mode. The uncoupled plasma resonance of the free conduction electrons is screened by the dielectric constant of the interband transitions and thus shifted to lower energies. In Fig. 9 the energy-loss function and the

FIG. 9. Reflectivity and energy-loss function of metallic SmS and of  $Gd_{0.94}S$ .

reflectivity of metallic SmS are shown over a reduced energy range and compared with  $\text{Gd}_{0.94}\text{S}$  for reasons which will be discussed in Sec. IX. Thus it becomes clear that the lustrous golden color of metallic SmS, just as in the case of GdS, is due to the coupled plasmon mode, which in turn induces the steep reflectivity edge in the visible part of the spectrum. It has been shown in Sec. IV that  $\epsilon_2$  can be decomposed into contributions from free electrons,  $\epsilon_2^f$ , and bound electrons,  $\epsilon_2^b$ , with the free-electron contribution being negligible for  $\omega > \omega_i$ , the onset of interband transitions at 3.1 eV. The decomposition of  $\epsilon_1 = \epsilon_1^f + \epsilon_1^b$  is based on the fact that we know  $\epsilon_2^b = \epsilon_2$  for  $\omega > \omega_i$ . Thus the contribution  $\epsilon_1^b$  of the bound electrons can be determined by performing the KK transformation of  $\epsilon_2^b$  in the region of interband transitions.<sup>11</sup> The resulting decomposition of  $\epsilon_1$  and  $\epsilon_2$  into free and bound contributions is shown in Fig. 10. In the absence of free electrons the sample is described by  $1 + \epsilon_1^b$ , which approaches the constant value  $\epsilon_\infty = 1 + \epsilon_\infty^b = 3.5$  with decreasing photon energy.  $\epsilon_1^f$  in Fig. 10 shows the well-known free-electron-like behavior, approaching a value of one for  $\omega \rightarrow \infty$ . The intersection  $\epsilon_1^f = 0$  at 4.6 eV gives the value of the true unperturbed plasma frequency  $\omega_p$  of the conduction electrons in the absence of interband transitions.  $\omega_p^2 = 4\pi N e^2 / m^*$  with  $N$  being the concentration of free electrons and  $m^*$  their effective mass. If we know the latter, we have a means to measure the carrier concentration and potentially obtain a measure of the valence fluctuation rate. This point will be taken up in Sec. IX.

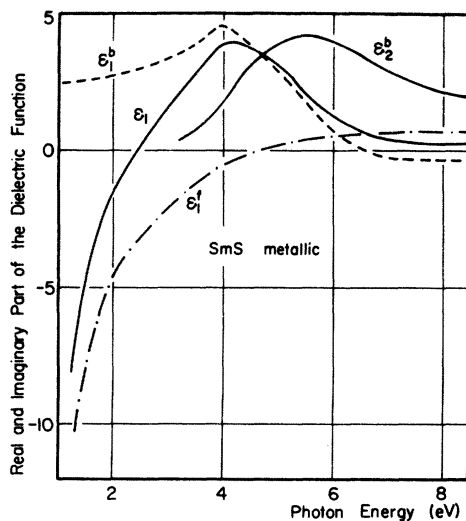


FIG. 10. Decomposition of the dielectric function into the free and bound electrons contribution.

## VI. THIN FILMS AND ABSORPTION COEFFICIENTS

The preparation of thin evaporated films of the Sm chalcogenides or polished thin platelets of single crystals permits the evaluation of the absorption edge, the multiplet splitting, the temperature and pressure shift of absorption peaks, and photoconductivity measurements. The absorption edge or the energy gap has been determined by transmission on single crystals of SmTe (0.62 eV),<sup>6</sup> SmSe (0.46 eV),<sup>6</sup> and SmS (0.065 eV).<sup>23</sup> Our measurements for SmTe and SmSe agree with the values of the absorption edge quoted above, and we have shown in addition that for all the Sm chalcogenides the absorption coefficient near the edge follows an Urbach rule, just as in the case of the Eu chalcogenides.<sup>36</sup> In the case of SmS, which has the smallest band gap, impurities may lead to a washed-out absorption, thus the edge could be at somewhat higher energies, probably at about 0.15 eV, as will be discussed in Sec. VII.

Transmission measurements on evaporated, semiconducting films of Sm chalcogenides,<sup>37-40</sup> and even on a polished, metallic film of SmS,<sup>32</sup> have been performed, usually in an energy range between 0.5 and 3.0 eV. In addition it has been shown that optical transitions near the absorption edge of SmSe lead to photoconductivity,<sup>41</sup> implying transitions to conduction-band states.

In Fig. 11 we show the computed absorption coefficient (as obtained from the KK analysis) of the semiconducting Sm chalcogenides up to 6 eV (between 6 and 12 eV the rather structureless absorption coefficient continues to rise to about  $10^6 \text{ cm}^{-1}$ ). These absorption coefficients are representative of single crystals and therefore avoid problems arising with the preparation and definition of thin films, but in general they are in good agreement with direct observations on thin films. In addition we show the computed absorption coefficient of our metallic SmS phase, which is in rather good agreement with the measurements on a polished SmS metallic film.<sup>32</sup> For comparison we also show the computed absorption coefficient of GdS crystals, which is in excellent agreement with transmission measurements on GdS films.<sup>42</sup> Especially, the drop of the absorption coefficient for photon energies less than about 1 eV is present in GdS and in SmS and has nothing to do with valence fluctuations in SmS, but is due to the frequency-dependent damping factor becoming larger than the frequency itself. This problem is discussed in Ref. 11. In Fig. 12 we show the measured optical density (proportional to the absorption coefficient) of a semiconducting SmS film for photon energies between 0.5 and 3.5 eV. The agreement with the curve in Fig. 11 and similar

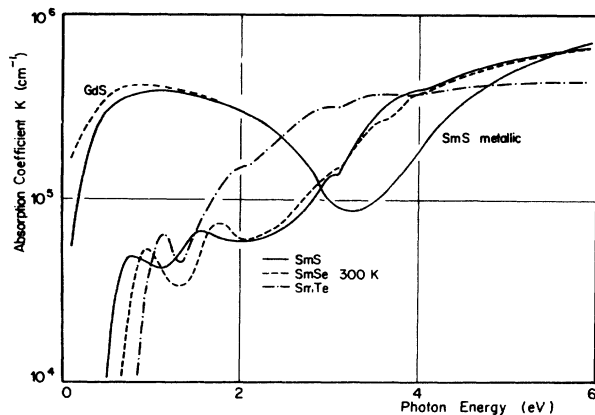


FIG. 11. Absorption coefficient of semiconducting SmS, SmSe, SmTe, and of metallic SmS and  $Gd_{0.94}S$ .

measurements of Holtzberg *et al.*<sup>39</sup> is very good, but in Figs. 11 and 12 the peak at 3.1 eV is clearly visible. Comparing Fig. 12 with Fig. 5 it becomes evident that the first two low-energy absorption peaks correspond to the  $4f^6 - 4f^5 ({}^6H_J, {}^6F_J)5d t_{2g}$  transitions, whereas the third absorption peak corresponds to the  $4f^6 - 4f^5 ({}^6H_J)5d e_g$  transition. From Fig. 12 we can again ascertain that the crystal-field splitting of the  $5d$  states,  $\Delta_{CF}$ , is 2.3 eV. We now have the possibility to apply hydrostatic pressure to the film (up to 1.5 kbar) and investigate the shift of the absorption peaks.<sup>40</sup> In addition, cooling the film to 4.2 K will apply lattice pressure ( $\approx 3.6$  kbar) owing to thermal contraction, which again will shift the absorption peaks.<sup>40</sup> Both types of measurements have been made at the photon energies of the peaks and points of inflection of an absorption curve and the energy shifts in meV/kbar are indicated in the figure. Our shift of the absorption edge of  $-10$  meV/kbar has recently been confirmed by Jayaraman *et al.*<sup>43</sup> It is

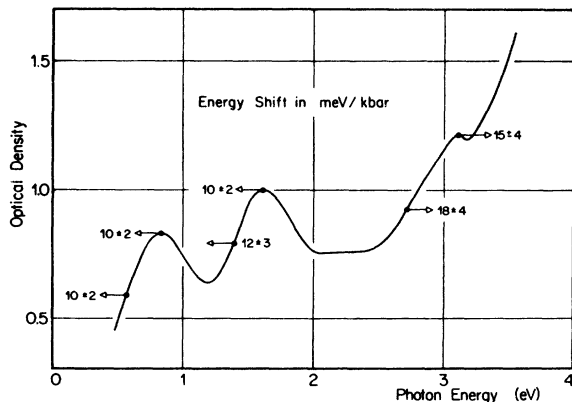


FIG. 12. Optical density of a semiconducting SmS film.

surprising that this value is about 25% larger than the value of the corresponding shift of the absorption edge of EuS, i.e.,  $-7.9$  meV/kbar.<sup>44</sup> But computing the deformation potential of SmS (to be precise, the *difference* between deformation potentials of  $4f$  and  $5d$  states) and using the reported bulk modulus,<sup>23,43</sup> one obtains within a few percent the same value as for EuS (4.7 and 4.8 eV, respectively). Thus the vicinity of a phase transition concomitant with a lattice collapse in SmS manifests itself even at normal pressure in a softening of the lattice compared with EuS.<sup>43</sup> The reason for this difference between SmS and EuS seems to be the strong  $5d$  admixture to the  $4f^6$  level of SmS because of its small energy gap.

In Fig. 12 it is shown that the first two  $5d t_{2g}$  peaks shift towards lower energy with pressure, whereas the third  $5d e_g$  peak shifts towards higher energy. In other words the crystal-field splitting  $\Delta_{CF}$  increases with pressure in such a way as to keep the energy difference of the  $4f^6$  and  $5d$  center of gravity constant. This is shown quantitatively in Fig. 12, since the degeneracy of the  $5d t_{2g}$  and  $5d e_g$  states is 3 and 2, respectively, and the ratio of their pressure shifts is 2:3. It is thus not the  $4f^6$  level which is rising in energy with pressure (otherwise one would observe only red shifts of all  $4f^6 - 5d$  transitions), but it is the crystal-field splitting of the  $5d$  states which is reducing the energy gap and driving the semiconductor-metal transition. With a pressure shift of  $-10$  meV/kbar and a critical pressure of 6.5 kbar the gap has been reduced by about 65 meV when the collapse of the lattice occurs with a first-order transition.

## VII. ELECTRICAL TRANSPORT PROPERTIES

It has been shown by Zhuze *et al.*<sup>45</sup> that the composition of SmS within its homogeneity range has a fundamental influence on the absolute value and the temperature dependence of the electrical conduction. Thus the room-temperature value of the conductivity may serve as a simple check of the stoichiometry of the sample in question. Our stoichiometric crystals of SmS (precision of chemical analysis  $\pm 0.5\%$ ) have a conductivity of  $37 (\Omega \text{ cm}^{-1})$  (using four-probe ac technique) in exact agreement with the published values.<sup>45</sup> In addition we have investigated the temperature dependence of the conductivity below room temperature.<sup>46</sup> Using  $\sigma = \sigma_0 \exp(-\Delta E/kT)$  we observed an activation energy of  $\Delta E = 60.6$  meV. The conductivity at 20 K is  $2.7 \times 10^{-6} (\Omega \text{ cm}^{-1})$ . According to Zhuze *et al.*<sup>45</sup> the activation energy is 0.2 eV for temperatures above 400 K, so it appears that at room temperature one is in an extrinsic conductivity range. In this connection it is suspicious that

owing to the critical pressure of 6.5 kbar of the semiconductor-metal transition, the energy gap has been reduced by 65 meV (see Sec. VI) and the activation energy of the defect is also about 60 meV. It would be very important to know whether this defect is coupled (example<sup>47</sup>: EuO:Gd) or decoupled [example: EuO with a deficiency of O (Ref. 48)] from the bottom of the conduction band and thus that under pressure it moves concomitant with the conduction band or not. On the other hand the observed long-wavelength optical absorption edge of 60 meV for SmS single crystals<sup>23,45</sup> may well be due to an impurity, thus being consistent with the thermal activation energy of the defect. It is then possible that the intrinsic energy gap in SmS is near 0.2 eV. About the same value is obtained considering the pressure dependence of the conductivity of SmS.<sup>6</sup> Up to the transition pressure of 6.5 kbar the conductivity increases by about 40% of its total change with pressure. Our measurements show that this corresponds to a reduction of the energy gap of 65 meV. The intrinsic gap is then estimated to be about  $0.065/0.4 = 0.160$  eV in good agreement with the high-temperature intrinsic thermal activation energy. In addition we have investigated the photoconductivity of the Sm chalcogenides<sup>49</sup> using intermittent and monochromatic illumination and a phase-sensitive detector. In the case of SmSe single crystals we find at 300 K a maximum in the photosensitivity (ratio of photoconductivity to incident light intensity) at about 0.9 eV, close to the lowest-energy absorption peak (see Fig. 11). For lower photon energies and at 20 K we observe a drop in the photosensitivity, reaching half maximum intensity at about 0.45 eV. This value yields the mobility gap,<sup>50</sup> which agrees with the optical gap. This coincidence has been established also for the Eu chalcogenides<sup>51</sup> and it shows that the  $4f^6 \rightarrow 4f^5 ({}^6H) 5d t_{2g}$  transition goes into a conduction band of primarily 5d character. A decay of an assumed excitonic state into a lower-lying 6s band can be practically excluded, because no experimental evidence of the rather strong, while parity allowed,  $4f^6 \rightarrow 6s$  optical transition below 0.46 eV has been observed. Besides, the thermal activation energy is in good agreement with the optical gap of the  $4f^6 \rightarrow 5d$  transition.<sup>6</sup>

### VIII. ELECTRONIC STRUCTURE AND ENERGY-LEVEL SCHEME

The experimental data discussed up to now, especially the dielectric functions in the interband energy region, should be sufficient for comparison with a band-structure calculation. There exists indeed a Korringa-Kohn-Rostoker calculation for

the Sm chalcogenides by Davis.<sup>52</sup> The essential results are that only in SmS the  $4f^6$  level is between the top of the  $3p^6$  valence band of sulfur and the minimum of the  $5d$  conduction band, whereas in SmSe and SmTe the  $4f^6$  level is below the top of the respective valence bands. In all cases, the 6s band  $\Gamma_1$  is above the minimum of the  $5d$  band at the X point of the Brillouin zone.

Another approach has been taken by Kaldis and Wachter,<sup>23</sup> who considered a tight-binding model for SmS, using ionization energies and affinities of cation and anion, the Madelung potential, and polarization energies. The crystal-field splitting of the  $5d$  conduction states has been taken to be the same as in EuS, since the lattice constants of EuS (5.96 Å) and SmS (5.97 Å) are practically the same. The essential result of this calculation was that the  $4f^6$  level of  $\text{Sm}^{2+}$  is about 1.5 eV higher in energy than the  $4f^7$  level of  $\text{Eu}^{2+}$ . This 1.5-eV energy difference corresponds to the difference of the third ionization energy between Eu (25.13 eV) and Sm (23.68 eV),<sup>53</sup> and it is a consequence of the fact that the half-filled  $4f^7$  shell of  $\text{Eu}^{2+}$  is much more tightly bound to the ion core than the less-than-half-filled shell of  $\text{Sm}^{2+}$ . The same model calculation for SmSe and SmTe also yields that the  $4f^6$  level of  $\text{Sm}^{2+}$  is between the top of the valence band and the bottom of the crystal-field-split  $5d$  conduction band, in contrast with the derivation of Davis.<sup>52</sup>

In Fig. 13 we show that the energy-level scheme of the Sm chalcogenides can be obtained from the scheme of the Eu chalcogenides. We plot the experimentally determined optical transition energies  $4f^n \rightarrow 5d t_{2g}$  and  $4f^n \rightarrow 5d e_g$  (taken from Figs. 5–7 and Ref. 51) and the band gap of the Eu,<sup>51</sup> and Sm, chalcogenides (taken from transmission on single crystals), respectively, as a function of the lattice constant. In the case of the Eu chalcogenides (left-hand scale) the final state of the  $4f^n \rightarrow 4f^{n-1}5d$  transition consists only of one ( ${}^7F_J$ ) multiplet, whereas in the Sm chalcogenides (right-hand scale) it consists of three ( ${}^6H_J$ ), ( ${}^6F_J$ ), ( ${}^6P_J$ ) multiplets; however, only the lowest-energy  ${}^6H_J$  transition is shown in the figure, the other final-state excitations are shifted as shown in Figs. 5–7. The zero of the energy scale is the  $4f^7$  and  $4f^6$  ground state of  $\text{Eu}^{2+}$  and  $\text{Sm}^{2+}$ , respectively. As already mentioned above, the  $4f^6$  level of  $\text{Sm}^{2+}$  is 1.5 eV above the  $4f^7$  level of  $\text{Eu}^{2+}$ , therefore, the energy scales in Fig. 13 are shifted by that amount. On these conditions one finds a perfect coincidence of all  $4f$ - $5d$  optical transitions of the Eu and Sm chalcogenides. The error bar for the band gap in SmS indicates the experimental uncertainty between 0.06 and 0.25 eV.

It is a remarkable property of this energy-level

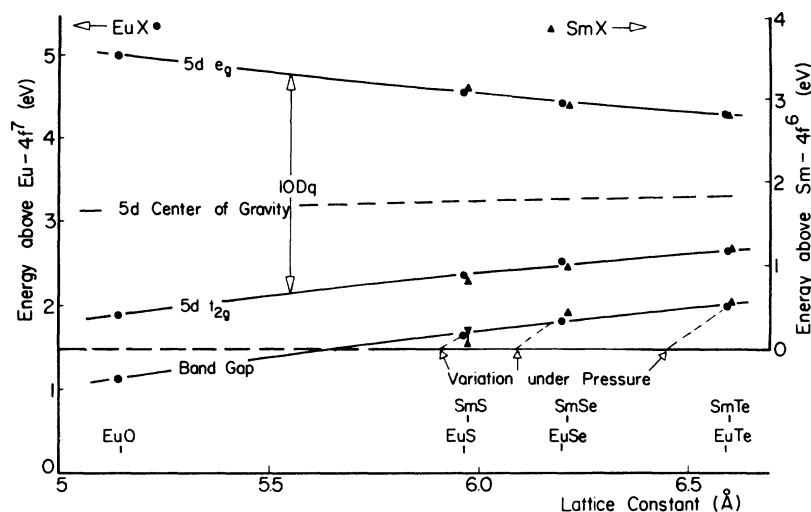


FIG. 13. Comparison of excitation energies between Sm and Eu chalcogenides, plotted vs the lattice constant.

scheme that the energy separation of the  $4f^n$  and  $5d$  center of gravity remains practically constant, as is to be expected in a more atomic-like model,<sup>23</sup> quite in contrast to the calculations of Davis.<sup>52</sup>

Another point of interest is the possible existence of  $\text{Sm}^{2+}\text{O}$  which, however, would have a "negative" band gap, as taken from Fig. 13. As a consequence, it can exist only in the form of  $\text{Sm}^{3+}\text{O}$  plus an electron, thus being a metal.

Figure 13 also indicates the mechanism of the semiconductor-metal transition of the Sm chalcogenides. Reduction of the lattice constant results in an increase of the  $5d$  crystal-field splitting  $10Dq$ . When the band gap thus has been driven to zero the transition occurs.<sup>40</sup> However, in actual pressure experiments one does not follow the band-gap line until its intersection with the zero of the energy scale. This variation would only be appropriate in chemical alloying experiments, where an exchange of the anion simultaneously changes the covalency of the compound. Instead, one observes experimentally a variation of the band gap with pressure as indicated in Fig. 13 by dashed lines. These are derived by computing from the pressure shift of the band gap<sup>40,43</sup> and the compressibility of the lattice<sup>23,43</sup> the change of the band gap per unit lattice contraction. It is found that the slope of the dashed lines in Fig. 13—the deformation potential—is constant for the Sm chalcogenides.

Now we may speculate why the semiconductor-metal transition in SmS is of first order and in SmSe and SmTe it is continuous. In all these compounds the metallic state consists of  $\text{Sm}^{(2+n)+}\text{X} + n$  electrons and the crystal structure is isostructural with the semiconducting rock-salt structure. The

total reduction in lattice constant during the transition is experimentally measured<sup>6</sup> or can be estimated by the reduction in ionic diameter of  $\text{Sm}^{2+}$  going to  $\text{Sm}^{3+}$ , assuming a hard-sphere model. If the reduction in band gap with pressure per concomitant reduction in lattice constant has the same value as the deformation potential (dashed line in Fig. 13), then the transition will be smooth and continuous. This is approximately the case in SmSe and SmTe.<sup>43</sup> If the misfit becomes too large as in SmS, where the closing of the band gap would only correspond to a reduction in lattice constant from 5.97 to 5.90 Å (see Fig. 13) instead of the observed one from 5.97 to 5.70 Å, then the lattice adjusts discontinuously in a first-order transition accompanied by hysteresis. Of course this is a consequence of the very small band gap in SmS to start with.

On the other hand, in the large band-gap materials EuS, EuSe, and EuTe (deformation potential about the same as for the Sm chalcogenides) the band gap is not yet closed when the lattice constant corresponds already to a  $\text{Eu}^{2+} \rightarrow \text{Eu}^{3+}$  transition. Therefore, the lattice first makes a structural change from fcc to bcc,<sup>43</sup> before the semiconductor-metal transition occurs.

In Fig. 14 we finally show a rough sketch of the density of states of the Sm chalcogenides, including also the anion  $p$  states. The curves are exact in energy, whereas the density of states is assumed parabolic and is only schematic. Band states are plotted to the right and initial and final localized states to the left. It is generally known that the dispersion of the  $5d$  conduction bands results in two pronounced density-of-states peaks, which in a more atomistic description are labeled  $t_{2g}$  and

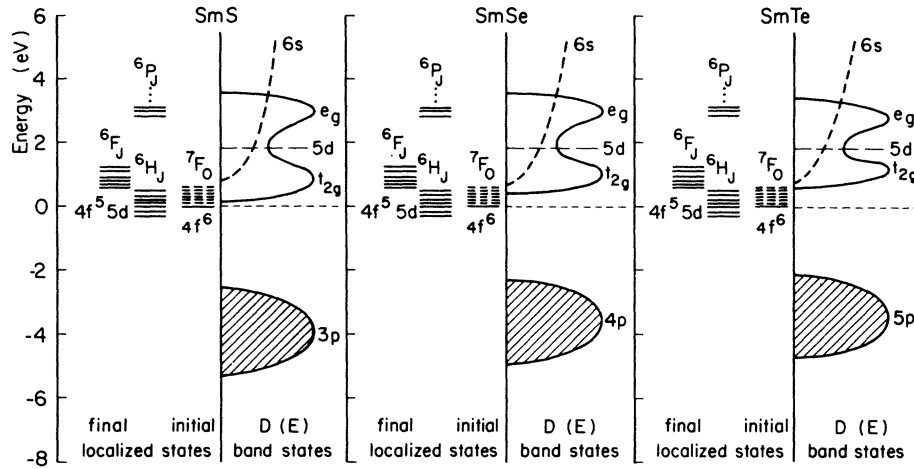


FIG. 14. Energy-level schemes of semiconducting SmS, SmSe, and SmTe.

$e_g$ . The energy separation  $p$ - $5d$   $t_{2g}$  (peak to peak) is with 4.8, 4.6, and 4.6 eV for SmS, SmSe, and SmTe, respectively, practically constant just as in the case of the Eu chalcogenides.<sup>51</sup> However, the energy separation of the  $p$ - $5d$  center of gravity or  $p$ - $4f^6$  is reduced in the same compound sequence. This is a manifestation of increasing covalency. The width of the valence bands is taken to be the same as in the corresponding Eu chalcogenides, where it has been determined by photoemission.<sup>54</sup> In contrast to EuSe and EuTe where the  $4f^7$  states are hybridized with the top of the valence band<sup>51,55</sup> making  $p$ -type conductivity possible, this is unlikely in SmSe and SmTe because the  $4f^6$  states are 1.5 eV higher in energy than the  $4f^7$  states in the Eu chalcogenides.

IX. METALLIC SmS AND THE PROBLEM OF VALENCE FLUCTUATIONS

The reflectivity data on metallic SmS (Figs. 2 and 9) and the dielectric functions (Fig. 8) now permit the derivation of an energy-level diagram. From the comparison of metallic SmS and  $Gd_{0.94}S$  in Fig. 9 it can be expected that the electronic structure of both compounds shows certain similarities,<sup>11,56</sup> which are indeed observed. In Fig. 15 we show the energy-level diagram of semiconducting (left-hand side) and metallic (right-hand side) SmS with reference to the Fermi energy  $E_F$ . Again, localized and band states are plotted separately. Just as in GdS the presence of about one free  $5d$  conduction electron per cation in SmS

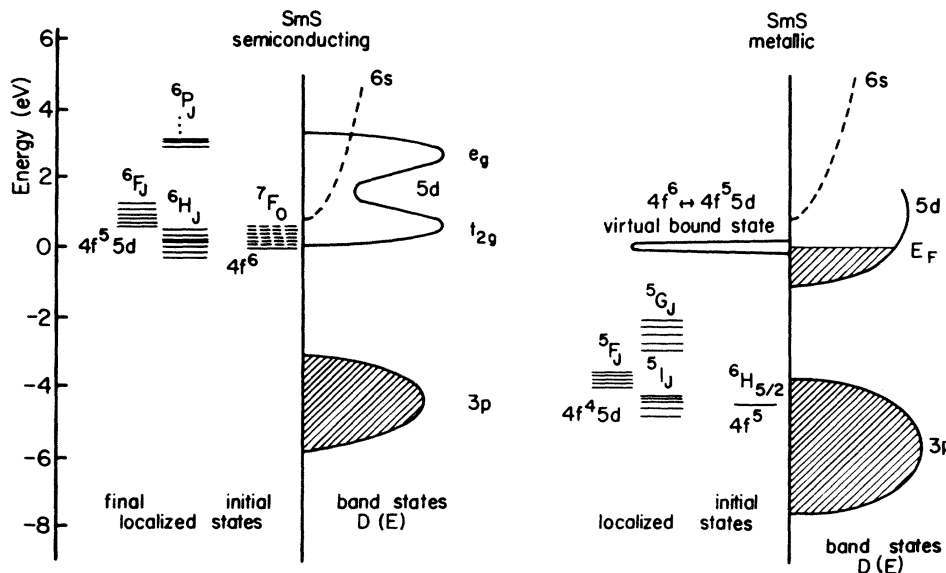


FIG. 15. Energy-level diagrams of semiconducting and metallic SmS.

also sufficiently screens the crystal-field splitting of the  $5d$  band. The free carriers fill the  $5d$  band up to the Fermi level. The energy of the bottom of the  $5d$  band is only an estimate, but similar values have been used as in GdS, where the energy difference between  $E_F$  and the bottom of the  $5d$  band has been observed by photoemission experiments.<sup>57</sup> From the low-energy limit of interband transitions, 3.1 eV, we derive the top of the  $3p^6$  valence band and from the peak of the interband transitions at 5.5 eV we obtain the maximum in the density of  $3p^6$  states, assuming a parabolic band shape. The width and the position of the valence band with respect to  $E_F$  are thus established and they are indeed in agreement with photoemission data on GdS.<sup>57</sup> The localized ground state  $4f^5$  ( ${}^6H_{5/2}$ ) of  $\text{Sm}^{3+}$  is observed about 4.5 eV below  $E_F$ , but final-state excitations, given also in the figure, are not resolved in the optical spectra, owing to the broad and rather structureless  $5d$  conduction band. The position below  $E_F$  of the  $4f^5$  state of  $\text{Sm}^{3+}$  in metallic SmS is found to be the same as in  $\text{Sm}_3\text{S}_4$ .<sup>58</sup>

The new feature of metallic SmS compared with GdS is the presence of a virtual bound state of original  $4f^6$  character right near or at  $E_F$ . This virtual state is basically localized but it may have a certain width in energy of possibly 0.01–0.1 eV, and it represents a high density of states. The possibility of valence fluctuations depends on the exact position in energy of this virtual state. If it is completely above  $E_F$ , SmS is purely trivalent and if it is completely below  $E_F$ , SmS is purely divalent, but as a consequence, the energy-level scheme is changing to the left-hand semiconducting diagram. Intermediate-valence states are thus possible and have been described in the literature.<sup>7,8,18-21</sup> The problem is to decide exactly the degree of mixed valence and fluctuation, if any at all.

It seems that in the literature one has settled for a value of an intermediate valence of 2.7. However, many of the measurements have been performed on chemically collapsed SmS,<sup>14-21,31</sup> but we think that this phase is not identical to the high-pressure phase of SmS owing to changes in covalency, chemical clustering, and incorporation of free electrons. Indeed there exist discrepancies between chemically and pressure-induced metallic SmS. SmS:Y changes from the golden metallic reflection at 300 K to a black surface at low temperatures,<sup>31</sup> quite in contrast to the high-pressure phase (Fig. 2 and Ref. 32). The fine structure of the reflectivity of SmS:Y is reminiscent of the simultaneous presence of  $\text{Sm}^{2+}$  reflectivity peaks. These are absent in the high-pressure phase of SmS (Fig. 2). The Mössbauer effect on SmS:Y

shows more divalent Sm than in the high-pressure phase.<sup>20,21</sup> Thus it may be safely concluded that chemically collapsed SmS has an intermediate valence near 2.7,<sup>18,19</sup> and that this value is less than the one in the high-pressure phase.

The lattice constant has always been used as best evidence for an intermediate valence in metallic SmS. The expected lattice constant for  $\text{Sm}^{3+}\text{S} + e$  has been interpolated from a plot of the lattice constants of trivalent rare-earth sulfides (e.g., Bucher *et al.*<sup>59</sup>) and found to be 5.62 Å. However, the experimentally observed lattice constant has been reported to be 5.70 Å,<sup>6</sup> and has been used to interpolate a mixed valence of 2.7.<sup>8</sup>

We now have performed an x-ray Bragg reflection on the polished golden surface of our metallic SmS single crystals. For the (100) face we have found two series of reflections of equal half-width, one corresponding to the semiconducting phase and one to the metallic surface. We take this as evidence that the polished metallic surface is also single crystalline. This important result supports our measurements on polished SmS as being representative for single crystals under hydrostatic pressure. On the other hand, the x-ray measurements permit a *differential* determination of the lattice constant of semiconducting and metallic SmS single crystals, observed at the same time in the same experiment. We obtain for metallic SmS a lattice constant of 5.68 Å and for semiconducting SmS the value given in Sec. II and compute an intermediate valence of 2.85.

We may expect, however, that x-ray experiments on large single crystals and with a true hydrostatic pressure of 6.5 kbar will yield an even smaller lattice constant (and thus an intermediate valence closer to three), because our measurements have been performed in the hysteresis region of the lattice collapse with pressures between 1.5 and 6.5 kbar.<sup>6</sup> Recently Bzhalava *et al.*<sup>26</sup> observed a lattice constant of only 5.66 Å for the collapsed metallic phase of SmS, yielding an intermediate valence of 2.90.

Another measure of the amount of valence fluctuations may be obtained by observing the plasma resonance of the free ( $5d$ ) conduction electrons. The uncoupled plasma resonance has been found at 4.6 eV (Sec. V) and the energy of this optical measurement is much larger than the hybridization energy (0.01 – 0.1 eV) of the virtual bound state. If the  $4f^6$ - $4f^55d$  virtual bound state in Fig. 15 intersects the Fermi level, we may assume that electrons scattered into this  $4f$  state are practically localized and acquire a very large effective mass. These electrons cannot take part in the high-frequency plasma resonance.<sup>60</sup> Therefore, the number  $N$  of  $5d$  conduction electrons taking

part in the plasma resonance divided by the number of cations directly yields the intermediate valence. Thus  $\omega_p^2 = 4\pi N e^2 / m^*$  ( $\hbar\omega_p = 4.6$  eV) is the equation to be solved and the problem is, of course, the effective mass  $m^*$ . Here we return to Fig. 9. We have often made use already of the similarities between metallic SmS and GdS. In GdS the simultaneous measurement of the plasma resonance and the Hall effect allowed the determination of  $m^* = 1.3m$ .<sup>11</sup> In Fig. 9 we compare metallic SmS with Gd<sub>0.94</sub>S because in both compounds the concentration of cations is the same. It is observed that the coupled plasma resonance at 2.45 eV is identical in both materials, therefore the color is identically golden. The reflectivity is similar for both compounds, except the small hump at 4.5 eV in SmS, and the 5d band structure is also similar. Therefore, if we use also for SmS an effective mass  $m^* = 1.3m$ , we obtain  $N = 2 \times 10^{22}$  cm<sup>-3</sup> and  $N/N_{\text{Sm}} = 0.9$ , which means 0.9 free electrons per cation. This yields an intermediate valence of 2.9 in good agreement with the interpolation from the lattice constant.

Therefore, we think that we have given good evidence that the high-pressure phase of SmS is indeed more trivalent than the chemically collapsed phase.

#### X. CONCLUSION

The measurement of the optical reflectivity over a very large energy range and its subsequent analysis in terms of the dielectric functions have enabled us to derive an energy-level scheme for the semiconducting phases of SmS, SmSe, and SmTe and for the metallic modification of SmS. Measurements of transmission on single crystals and

thin films have confirmed the polaronic nature of the semiconducting Sm chalcogenides, and have shown that the 4f<sup>6</sup>-5d t<sub>2g</sub> energy gaps are reduced by 1.5 eV as compared with the corresponding Eu chalcogenides. Just as in the case of the Eu chalcogenides, the onset of the optical 4f<sup>6</sup> 5d absorption is accompanied by photoconduction, indicating transitions into a conduction band. The rather small energy gaps of the Sm chalcogenides (about 0.15 eV for SmS) shift pressure-induced semiconductor-metal transitions into a more accessible pressure range. The mechanism of the phase transition seems to be the crystal-field splitting of the 5d conduction band which becomes enhanced by a lattice compression and is driving the energy gap of 4f<sup>6</sup>-5d t<sub>2g</sub> towards zero. The subsequent delocalization of a 4f electron yields a free 5d conduction electron. We could show that the chemically induced metallic phase of SmS is not the same as the pressure-induced phase, and that the latter is more trivalent than the former. The agreement between the intermediate valence computed from the lattice constant of the high-pressure phase and the plasma resonance of the free conduction electrons is reassuring and yields a valence of 2.9. However, the possible influence of defects, like sulfur vacancies, on the pressure-induced phase transition of SmS cannot be ruled out completely, because after all, at 300 K one is in an extrinsic conduction regime.

#### ACKNOWLEDGMENTS

The authors are grateful to J. Müller, and A. Ernst for technical assistance. The financial support of the Swiss Science Foundation is gratefully acknowledged.

<sup>1</sup>M. Picon and M. Patrie, C. R. Acad. Sci. **242**, 1321 (1956).

<sup>2</sup>M. Picon, L. Domange, I. Flahut, M. Guittard, and M. Patrie, Bull. Soc. Chim. **2**, 221 (1960).

<sup>3</sup>*Rare Earth Research*, edited by E. V. Kleber (New York, 1961), p. 225.

<sup>4</sup>R. Didchenko, F. P. Gortsema, and J. W. McClure, J. Appl. Phys. **24**, 863 (1963).

<sup>5</sup>V. P. Zhuze, A. V. Golubkov, E. V. Goncharova, T. I. Komarova, and V. M. Sergeeva, Fiz. Tver. Tela **6**, 268 (1964) [Sov. Phys.-Solid State **6**, 213 (1964)].

<sup>6</sup>A. Jayaraman, V. Narayanamurti, E. Bucher, and R. G. Maines, Phys. Rev. Lett. **25**, 368, 1430 (1970).

<sup>7</sup>L. L. Hirst, Phys. Kondens. Mater. **11**, 255 (1970).

<sup>8</sup>M. B. Maple and D. Wohlleben, Phys. Rev. Lett. **27**, 511 (1971).

<sup>9</sup>W. Beckenbaugh, G. Güntherodt, R. Hauger, E. Kaldis, J. P. Kopp, and P. Wachter, AIP Conf. Proc. **18**, 540 (1974).

<sup>10</sup>G. Güntherodt and P. Wachter, AIP Conf. Proc. **18**, 1034 (1974).

<sup>11</sup>W. Beckenbaugh, J. Evers, G. Güntherodt, E. Kaldis, and P. Wachter, J. Phys. Chem. Solids **36**, 239 (1975).

<sup>12</sup>R. Hauger, E. Kaldis, G. von Schulthess, P. Wachter, and Ch. Zürcher, AIP Conf. Proc. **24**, 46 (1975).

<sup>13</sup>R. Hauger, E. Kaldis, G. von Schulthess, P. Wachter, and Ch. Zürcher, J. Magnet. Mater. **3**, 103 (1976).

<sup>14</sup>F. Mehran, J. B. Torrance, and F. Holtzberg, Phys. Rev. B **8**, 1268 (1973).

<sup>15</sup>F. Holtzberg, AIP Conf. Proc. **18**, 478 (1974).

<sup>16</sup>A. Jayaraman, E. Bucher, P. D. Dernier, and L. D. Longinotti, Phys. Rev. Lett. **31**, 700 (1973).

<sup>17</sup>A. Jayaraman, P. Dernier, and L. D. Longinotti, Phys. Rev. B **11**, 2783 (1975).

<sup>18</sup>R. A. Pollak, F. Holtzberg, J. L. Freeouf, and D. E. Eastman, Phys. Rev. Lett. **33**, 820 (1974).

<sup>19</sup>M. Campagna, E. Bucher, G. K. Wertheim, and L. D.

- Longinotti, Proceedings of the 11th Rare Earth Conference, Traverse City, 53 (1974) (unpublished); Phys. Rev. Lett. **33**, 165 (1974).
- <sup>20</sup>J. M. D. Coey and S. K. Ghatak, International Conference on Mössbauer Spectroscopy, Cracow, Poland (1975) (unpublished).
- <sup>21</sup>J. M. D. Coey, S. K. Ghatak, and F. Holtzberg, AIP Conf. Proc. **24**, 38 (1975).
- <sup>22</sup>E. Kaldis, in *Crystal Growth, Theory and Techniques*, edited by C. H. L. Goodman (Plenum, New York, 1974), Vol. 1.
- <sup>23</sup>E. Kaldis and P. Wachter, Solid State Commun. **11**, 907 (1972).
- <sup>24</sup>D. W. Pohl, R. Badertscher, K. A. Müller, and P. Wachter, Appl. Opt. **13**, 95 (1974).
- <sup>25</sup>V. V. Kaminskii, A. I. Shelykh, T. T. Dedegkaev, T. B. Zhukova, S. G. Shul'man, and I. A. Smirnov, Fiz. Tver. Tela **17**, 1546 (1975) [Sov. Phys.-Solid State **17**, 1015, (1975)].
- <sup>26</sup>T. L. Bzhalava, S. G. Shul'man, T. T. Dedegkaev, T. B. Zhukova, and I. A. Smirnov, Phys. Lett. A **55**, 161 (1975).
- <sup>27</sup>G. Güntherodt, in *Festkörperprobleme (Advances in Solid State Physics)*, Vol. XVI, edited by J. Treusch (Vieweg, Braunschweig, 1976), p. 95.
- <sup>28</sup>J. L. Kirk, K. Vedam, V. Narayanamurti, A. Jayaraman, and E. Bucher, Phys. Rev. B **6**, 3023 (1972).
- <sup>29</sup>J. D. Axe, J. Phys. Chem. Solids **30**, 1403 (1969).
- <sup>30</sup>G. D. Holah, J. S. Webb, R. B. Dennis, and C. R. Pidgeon, Solid State Commun. **13**, 209 (1973).
- <sup>31</sup>G. Güntherodt and F. Holtzberg, AIP Conf. Proc. **24**, 36 (1975).
- <sup>32</sup>D. W. Pohl, R. Jaggi, K. Gisler, and H. Weibel, Solid State Commun. **17**, 705 (1975).
- <sup>33</sup>G. Güntherodt, Phys. Kondens. Mater. **18**, 37 (1974).
- <sup>34</sup>P. A. Cox, Y. Baer, and C. K. Jørgensen, Chem. Phys. Lett. **22**, 433 (1973).
- <sup>35</sup>G. H. Dieke, *Spectra and Energy Levels of Rare Earth Ions in Crystals*, edited by H. M. and H. Crosswhite (Interscience, New York, 1968).
- <sup>36</sup>J. Schoenes, Z. Phys. B **20**, 345 (1975).
- <sup>37</sup>R. Suryanarayanan, C. Paparoditis, and J. Ferré, Rare Earth and Actinides, Durham, Conf. Digest No. 3, 210 (1971) Proc. Int. Conf. Thin Films, Cannes, Levide Suppl. **147** (1970).
- <sup>38</sup>E. Bucher, V. Narayanamurti, and A. Jayaraman, J. Appl. Phys. **42**, 1741 (1971).
- <sup>39</sup>F. Holtzberg and J. B. Torrance, AIP Conf. Proc. **5**, 860 (1972).
- <sup>40</sup>B. Batlogg, J. Schoenes, and P. Wachter, Phys. Lett. A **49**, 13 (1974).
- <sup>41</sup>R. Suryanarayanan and C. Paparoditis, Phys. Lett. A **42**, 373 (1973).
- <sup>42</sup>J. Schoenes, this laboratory (unpublished).
- <sup>43</sup>A. Jayaraman, P. Dernier, and L. D. Longinotti, Phys. Rev. B **11**, 2783 (1975).
- <sup>44</sup>P. Wachter, Solid State Commun. **7**, 693 (1969).
- <sup>45</sup>V. P. Zhuze, E. V. Goncharova, N. F. Kartenko, T. I. Komarova, L. S. Parfeneva, V. M. Sergeeva, and I. S. Smirnov, Phys. Status Solidi A **18**, 63 (1973).
- <sup>46</sup>K. Neufeld, Master's Thesis ETH (unpublished).
- <sup>47</sup>J. Schoenes and P. Wachter, Phys. Rev. B **9**, 3097 (1974).
- <sup>48</sup>M. R. Oliver, J. O. Dimmock, and T. B. Reed, IBM J. Res. Dev. **14**, 276 (1970).
- <sup>49</sup>B. Batlogg, U. Müller, and P. Wachter (unpublished).
- <sup>50</sup>T. S. Moss, *Photoconductivity in the Elements* (Academic, New York, 1952).
- <sup>51</sup>P. Wachter, Crit. Rev. Solid State Sci. **3**, 189 (1972).
- <sup>52</sup>H. L. Davis, Proceedings of the 9th Rare Earth Conference, Blacksburry, Virginia, p. 3, (1971) (unpublished).
- <sup>53</sup>L. R. Morss, J. Phys. Chem. **75**, 393 (1971).
- <sup>54</sup>D. E. Eastman, F. Holtzberg, S. Methfessel, Phys. Rev. Lett. **23**, 226 (1969).
- <sup>55</sup>P. Wachter, Z. Angew. Phys. **32**, 171 (1971).
- <sup>56</sup>G. Güntherodt and F. Wachter, Proceedings of the 11th Rare Earth Conference, Traverse City, p. 820 (1974) (unpublished).
- <sup>57</sup>D. E. Eastman and M. Kuznietz, J. Appl. Phys. **42**, 1396 (1971).
- <sup>58</sup>B. Batlogg, E. Kaldis, A. Schlegel, G. von Schulthess, and P. Wachter, Solid State Commun., **19**, 673 (1976); J. Magnet. Mater. **3**, 96 (1976).
- <sup>59</sup>E. Bucher, K. Andres, F. J. Di Salvo, J. P. Maita, A. C. Gossard, A. S. Cooper, and G. W. Hull, Jr., Phys. Rev. B **11**, 500 (1975).
- <sup>60</sup>R. W. Ward, B. P. Clayman, and T. M. Rice, Solid State Commun. **17**, 1297 (1975).